may contribute substantially to coral bleaching. UV-induced bleaching happens rapidly (within three weeks) and can occur in the absence of raised seawater temperatures. Second, concentrations of MAAs within the coral–algal symbiosis cannot be augmented at a rate sufficient to counter UV light increases resulting from rapid changes in water-column conditions. Third, coral bleaching induced by UV radiation results from reductions in zooxanthella densities rather than the combined effects of zooxanthellae expulsion and decreases in chlorophyll concentrations per algal cell, as has been noted in temperature-related bleaching[10].

Verification that increased UV radiation induces coral bleaching in the absence of abnormally high seawater temperatures raises additional concerns regarding potential climate change and coral stress. Increases in UV intensity due to anthropogenic ozone depletion will be minimal at low latitudes and should not be a factor in bleaching[22], but an increase in the frequency or duration of exceptionally calm (doldrums) and clear water conditions, which accompany such large-scale climatic phenomena as El Niño/Southern Oscillation, for example, could lead to greater penetration of UV radiation on coral reefs and thus to an increased potential for UV-induced bleaching[2]. □

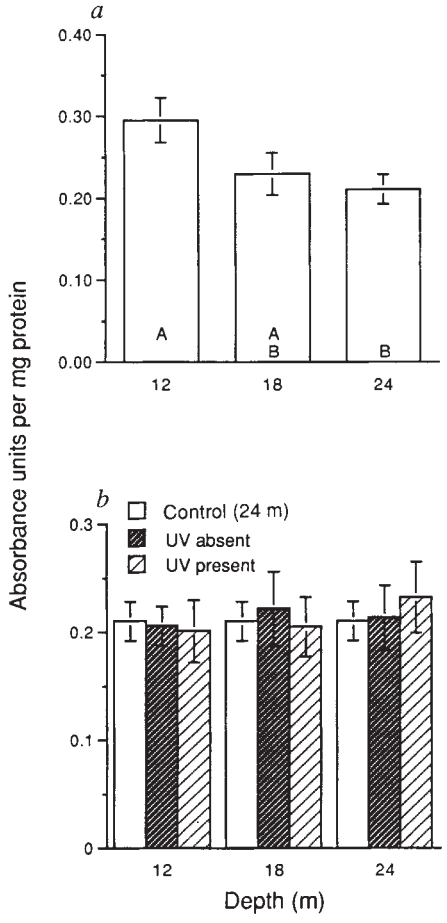

FIG. 3 Absorbance at 320 nm by mycosporine-like amino acids (MAAs) extracted from colonies of *M. annularis*. *a*, Absorbance units per mg soluble coral protein for unmanipulated colonies collected from 12, 18 and 24 m depth. Values represent means (±s.e.) of 10 colonies at each depth. Bars labelled on the interior with the same letter (A or B) were not significantly different at $P=0.05$ (Tukey's HSD test). *b*, Absorbance units per mg soluble coral protein for colonies transplanted from 24 m to 24, 18 and 12 m depth. Treatments are described in Fig. 2 legend. Bars represent means (±s.e.) of 10 colonies. No significant differences in absorbance were detected between treatments at each depth (one-way ANOVA, $P>0.05$ in each case). In both *a* and *b*, MAAs were extracted from 1–2-cm^2 sections of coral tissue with three 5-ml volumes of 20% tetrahydrofuran in methanol. The initial extraction was for 24 h at 4 °C, and the other two were for 5 min under sonication in an ice bath. To detect MAAs, solutions were scanned between 280 and 400 nm on a Milton Roy Spectronic 3000 diode array spectrophotometer. *M. annularis* colonies all had a peak absorbance at 320 nm. Soluble protein was determined after extraction of MAAs as for Fig. 2.

Received 11 February; accepted 23 July 1993.

1. Glynn, P. W. *Trends Ecol. Evol.* **6,** 175–179 (1991).
2. Glynn, P. W. *Coral Reefs* **12,** 1–17 (1993).
3. Jaap, W. C. *Bull. mar. Sci.* **29,** 414–422 (1979).
4. Glynn, P. W. *Environ. Conserv.* **11,** 133–146 (1984).
5. Atwood, D. K. *et al. Proc. Assoc. mar. Lab. Caribbean* **21,** 47 (1988).
6. Glynn, P. W. *A. Rev. Ecol. Syst.* **19,** 309–345 (1988).
7. Porter, J. W., Fitt, W., Spero, H., Rogers, C. & White, M. *Proc. natn. Acad. Sci. U.S.A.* **86,** 9342–9346 (1989).
8. Cook, C. B. *et al. Coral Reefs* **9,** 45–49 (1990).
9. Jokiel, P. L. & Coles, S. *Coral Reefs* **8,** 155–162 (1990).
10. Glynn, P. W. & D'Croz, L. *Coral Reefs* **8,** 181–191 (1990).
11. Goenaga, C., Vicente, V. P. & Armstrong, R. A. *Carib. J. Sci.* **25,** 59–65 (1989).
12. Atwood, D. K., Hendee, J. & Mendez, A. *Bull. mar. Sci.* **51,** 118–130 (1992).
13. Williams, E. H. & Bunkley-Williams, L. *Atoll. Res. Bull.* **335,** 1–71 (1990).
14. Marra, J. *Mar. Biol.* **46,** 203–208 (1978).
15. Neale, P. J. in *Photoinhibition* (eds Kyle, D., Osmond, C. & Arntzen, C.) 35–65 (Elsevier, Amsterdam, 1987).
16. Jokiel, P. L. & York, R. H. *Bull. Mar. Sci.* **32,** 301–315 (1982).
17. Dunlap, W. C. & Chalker, B. E. *Coral Reefs* **5,** 155–159 (1986).
18. Gleason, D. F. *Limnol. Oceanogr.* (in the press).
19. Smith, R. C. & Baker, *K. Appl. Optics* **20,** 177–184 (1981).
20. Gibson, J. H. *Justification and Criteria for the Monitoring of Ultraviolet Radiation* (National Atmospheric Deposition Program/National Trends Network, Colorado State Univ., Fort Collins, 1991).
21. Smith, R. C. & Baker, K. S. *Photochem. Photobiol.* **29,** 311–323 (1979).
22. Stolarski, R. R. *et al. Science.* **256,** 342–349 (1992).
23. Wellington, G. M. *Oecologia* **52,** 311–320 (1982).
24. Jeffrey, S. W. & Humphrey, G. *Biochem. physiol. Pfl.* **167,** 191–194 (1975).
25. Bradford, M. M. *Analyt. Biochem.* **72,** 248–254 (1976).
26. Marsh, J. A. *Ecology* **51,** 255–263 (1970).

ACKNOWLEDGEMENTS. We thank D. Gerace and the Bahamian Field Station for logistical support, and L. Gutierrez, M. Hill and especially J. Schmerfeld for help in the field and laboratory. Supported by the NSF and the National Oceanic and Atmospheric Administration's National Undersea Research Center at the University of North Carolina at Wilmington.

Reverse transduction measured in the isolated cochlea by laser Michelson interferometry

Fabio Mammano & Jonathan F. Ashmore*

Department of Physiology, School of Medical Sciences, University Walk, Bristol BS8 1TD, UK

IT is thought that the sensitivity of mammalian hearing depends on amplification of the incoming sound within the cochlea by a select population of sensory cells, the outer hair cells. It has been suggested that these cells sense displacements and feedback forces which enhance the basilar membrane motion by reducing the inherent damping of the cochlear partition[1–7]. In support of this hypothesis, outer hair cells show membrane-potential-induced length changes[1–3] at acoustic rates. This process has been termed 'reverse transduction'. For amplification, the forces should be large enough to move the basilar membrane. Using a displacement-sensitive interferometer[8], we tested this hypothesis in an isolated cochlea while stimulating the outer hair cells with current passed across the partition. We show here that the cochlear partition distorts under the action of electrically driven hair cell length changes and produces place-specific vibration of the basilar membrane of a magnitude comparable to that observed near auditory threshold (about 1 nm). Such measurements supply direct evidence that cochlear amplification arises from the properties of the outer hair cell population.

* To whom correspondence should be addressed.

Under visual control, focal electrical stimuli were applied across the organ of Corti by creating a diverging field between a 5 μm-diameter stimulus pipette placed in scala media and an indifferent earth below the isolated cochlea. To obtain access to the third turn of the cochlear spiral, about 11 mm from the stapes, the cochlea was opened and Reissner's membrane gently peeled away. Nanometre displacements of the intact cochlear partition were detected at several positions on the partition surface facing scala media using a displacement-sensitive laser interferometer (Fig. 1*a*). Placing the pipette tip near the outer hair cells maximized the size of the responses (which were generally too small to be measured if the pipette tip was displaced radially by more than 500 μm from the outermost row of cells).

Figures 1*b* and 2 show responses of the basilar membrane and those of the reticular lamina (the top surface of the organ of Corti) near the outer hair cells at the same site in cochlear turn 3. The difference in current flowing into the pipette through the outer hair cells and through extracellular space resulted in a net cell depolarization (Fig. 2*a*) and produced basilar membrane step displacements towards the scala media (Fig. 2*b*), whereas the reticular lamina moved in the opposite direction (Fig. 2*c*). The basilar membrane displacements were accompanied by damped oscillations. The motion of the reticular lamina was 5–10 times larger (Figs 1*b* and 2*d*) and generally showed an over-damped response (Figs 1*b* and 2*c*). The polarity of these responses was reversed by reversing the stimulus current. The steady displacement of the structures indicate that the forces generated by electrical stimuli were large enough to overcome the partition stiffness and to distort its geometry (Fig. 1*c*). There was no significant difference in basilar membrane responses when the experiments were conducted at 37 °C (data not shown).

Although no cochlear cells other than the outer hair cells have been reported to respond mechanically to electrical stimuli, we attempted to single out the origin of the forces elicited by extrinsic current by pharmacological techniques. It is known that salicylate (aspirin) can induce a reversible 20–27 decibel rise in the threshold of response for cochlear nerve fibres at their characteristic frequency[12,13] and suppress spontaneous otoacoustic emissions[14]. Superfusion with 10 mM sodium salicylate reversibly diminishes electromotility in isolated outer hair cells[15]. Figure 3 shows that, on introducing an iso-osmotic medium containing 10 mM sodium salicylate for 5 min, a 50% reduction in the size of the basilar membrane response was observed. The response recovered within 12 min. Gadolinium, a reversible blocker of outer hair cell motility[16], was not effective at 1 mM, possibly because of its limited diffusion into the organ of Corti.

These results have implications for cochlear mechanics. The microelectrode recordings show that outer hair cells depolarize, and hence shorten[3], in response to negative current pulses. As outer hair cells are strategically inserted between the basilar membrane and the reticular lamina, a change in their resting length would alter their axial tension. Therefore the simplest explanation of our findings is that the organ of Corti alters its dimensions when the outer hair cells change length. As the mean sensitivity of outer hair cells to extrinsic current was −24.8 V/A ($n=5$, range −15.3 to −43.2 V/A), 100 μA would have altered the membrane potential by 2.5 mV, which at the measured membrane potential would cause isolated outer hair cells to change length by 50 nm[3,17]. The corresponding differential displacement of the cochlear surface by 20 nm implies that the assembly of outer hair cells has a mechanical impedance which numerically matches that of the rest of the cochlear partition. We thus conclude that outer-hair-cell length changes may be functionally less constrained by the surrounding cells than cochlear structure would suggest.

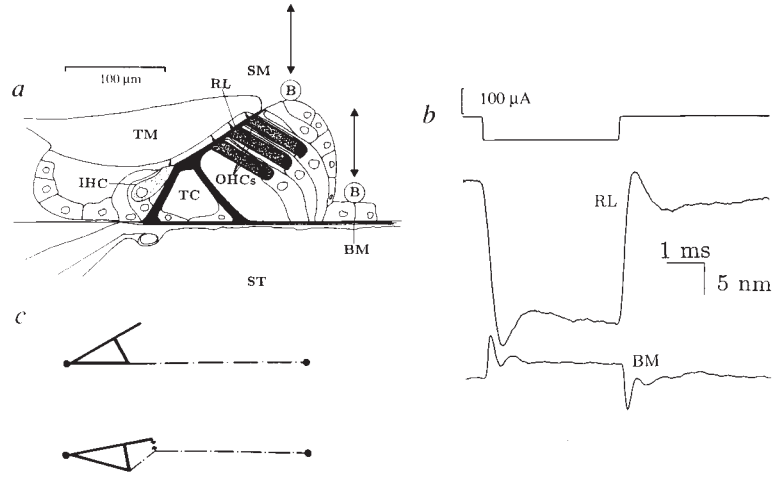

FIG. 1 Schematic drawing of the cochlear partition cross-section, showing the organ of Corti and the position of the measurements. *a*, Location of the beads (B) where displacement measurements were made is indicated by double vertical arrows. The partition separates scala media (SM) from scala tympani (ST); OHC (IHC), outer (inner) hair cells; TM, tectorial membrane; TC, triangle of Corti, formed by the inner and outer pillar cells. *b*, Sample responses from the reticular lamina, (RL, upper trace) and the basilar membrane, (BM, pars pectinata, lower trace) are also shown. For all traces shown in this paper, upward (downward) deflections indicate displacements towards scala media (scala tympani). Note different amplitudes of the motions. After the initial transient following the step onset, both responses settled to a new steady level, but in opposite directions. This implies that the geometry of the partition as well as the basilar membrane tension are altered by internal forces acting within the partition. *c*, Hypothesized rotation of the TC (heavy lines) around pivot beneath the IHC and induced by OHC shortening.

METHODS. Adult guinea-pigs (200–300 g) were killed by rapid cervical dislocation. After isolating the temporal bone, the bulla was opened and firmly held in a perspex chamber perfused with oxygenated L-15 medium (Gibco) adjusted to pH 7.35 and osmolarity 317 ± 2 mosM. The cochlear partition was observed under low magnification from scala media by gently scraping away the bony wall of the cochlea and removing Reissner's membrane. Interferometric measurements were made with a × 40 0.75 NA water-immersion objective (Zeiss). The Michelson interferometer[8] was illuminated by a stabilized He–Ne 1 mW laser (Model 200, Coherent, Cambridge, UK) and consisted of a fixed reference path and one path in which the beam was reflected back through the objective from aluminium sputter-coated 10 μM glass beads (Mo-Sci Corporation, Rolla, MO, USA) which were allowed to settle on the partition. The intensity of the recombined interfering beams was measured by a photodiode with a flat response from DC to 20 kHz. The diode output was sampled at 31 kHz and averaged 100 times. The stimulus repetition rate was either 8 or 21 Hz. The interferometer was kept in quadrature under software control. Optimally adjusted, the interferometer was capable of measuring static displacements of the spherical beads. Small radial rocking motions of the beads could cause changes greater than 3 nm in the baseline and in these cases the data were discarded. Displacements were calibrated for each averaging cycle by displacing the reference mirror of the interferometer by a fixed distance, usually 160 nm. Current generated by a controlled stimulator was injected through a micropipette (diameter 5 μm) filled with agar–saline to eliminate fluid bulk flow. Whenever necessary, the stimulator wave-shaping circuitry was used to compensate for the stray capacitance of the pipette so as to reduce the step rise time to less than 20 μs. The current was measured with a virtual ground circuit. Downward current traces correspond to current flowing into the pipette. Temperature, 24–28 °C.

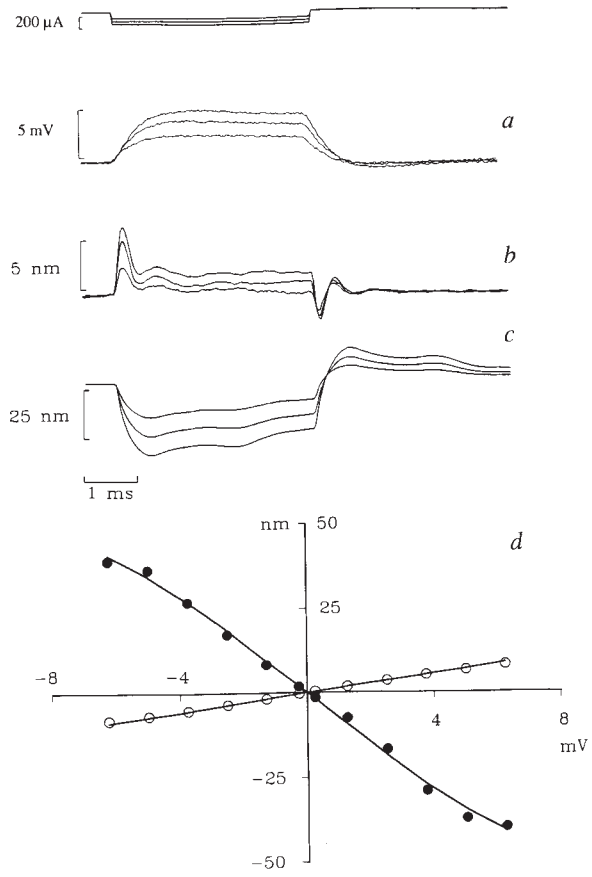

FIG. 2 The cochlear partition moves under millivolt changes of hair membrane potential. *a*, Changes in membrane potential induced by current steps in an outer hair cell located underneath the stimulus pipette. Upward deflections indicate cell depolarization. Resting potential, −19 mV. The slowed time course of the intracellular responses is due to the high resistance microelectrode time constant[9] (1 ms). *b*, Displacements of the basilar membrane elicited by current steps during the same experiment. *c*, Displacement of the reticular lamina in the same cochlea at the same site of *b*. *d*, Voltage-displacement characteristics. Open symbols, basilar membrane; filled symbols, reticular lamina. Abscissae show cell membrane potential changes obtained by converting applied current levels with a sensitivity factor of 25 V/A. Cell depolarization corresponds to motion of the basilar membrane towards scala media and motion of the reticular lamina towards scala tympani. Both responses began to saturate with membrane potential changes in excess of 5 mV (equivalent to 200 μA stimulus).

METHODS. Microlectrodes were pulled from 1 mm (outside diameter) fibre-filled glass tubing (Clark Electromedical, UK) on a P-87 puller (Sutter Instruments) and had a resistance of 150–200 megohms in the bath when filled with 3 M potassium acetate. After completing a series of interferometric measurements, the tectorial membrane was removed with a finely etched tungsten needle held in a manipulator (Singer) while the stimulus pipette was left in place. Outer hair cells in the proximity of the recording site were impaled from the reticular lamina side under direct visual control and the series of stimulus pulses repeated twice for each cell, once with the microelectrode inside and once just above the cell. The microelectrode amplifier output was sampled at 31 kHz and averaged 60 times, (repetition rate 21 Hz). Changes in membrane potential were measured by subtracting the recordings taken inside from those taken outside each cell. Control experiments obtained by passing the electrode through RL showed that the potential difference across RL was negligible (about 0.5 mV at 200 μA; data not shown). This was a consequence of placing the cochlea in bathing medium which provides a low-resistance pathway to the extracellular current flow. The recorded potential difference between the cell interior and the surface of RL is thus a good estimate of the potential of the basolateral membrane where the OHC motors are located[2]. The average resting membrane potential was -19.2 ± 4.7 mV (s.d., $n=5$). Cells with a resting potential more positive than −14 mV were discarded. Depolarized resting potentials arise when the apical outer hair cell surface is exposed to artificial perilymph following the removal of Reissner's membrane[10]; electromotile responses are, however, insensitive to such altered bathing medium on this surface[11].

The antiphase motion of the basilar membrane and the reticular lamina show that each transverse section of the cochlear partition possesses at least two degrees of freedom, so that the top and bottom of the organ of Corti move independently. This represents a departure from classical models of cochlear excitation (ref. 18 for example), which regard the organ of Corti as a single-hinged and rigid structure, but is consistent with those that recognize multiple structures of the partition[19]. As proposed in a recent model[20], if one mechanical degree of freedom is associated with the basilar membrane pars pectinata and a second with the rigid framework formed by the triangle of Corti and the reticular lamina, the triangle of Corti would rotate towards scala tympani (downwards, Fig. 1) if the outer hair cells shorten and pull the reticular lamina towards the basilar membrane (Fig. 1*c*). Conversely, the triangle would rotate towards scala media (upwards) if the cells elongate. In both cases, measuring points on the basilar membrane and reticular lamina would move in antiphase when the cells are stimulated.

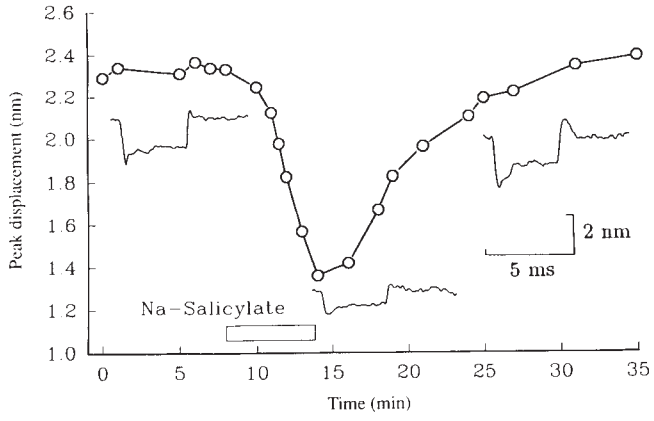

FIG. 3 Partition motion is reduced by salicylate. 10 mM sodium salicylate (bar) in the perfusion medium was added for the time indicated. The response amplitude (and the tuning quality factor) were reduced by 50%.

METHODS. The solution in the 1 ml chamber was continuously changed (2 ml min^{-1}). The estimated dead-time for solution change was about 2 min. To avoid tissue swelling, all solutions were iso-osmotic with control.

In such a scheme, the mechanical behaviour of each transverse section can be modelled if we note that the triangle of Corti/basilar membrane system (Fig. 1*a*, *c*) can be represented by a pair of masses m_1, m_2 held by (damped) springs with stiffness k_1, k_2, respectively. If these resonant systems are excited simultaneously by equal and opposite forces (applied by the outer hair cells) they would move by amounts inversely proportional to the associated spring stiffness. If the masses are comparable (that is $m_1 \approx m_2$), the ratio of the natural frequency of the oscillators would be proportional to $(k_1/k_2)^{0.5}$. The basilar membrane was tuned to a frequency of 2.3 ± 0.15 kHz (s.d., $n=11$) about 11 mm from the cochlear base, in agreement with published cochlear frequency maps[21]. The responses of the reticular lamina at the same site had a frequency of 1.0 ± 0.15 kHz (s.d., $n=11$). This suggests that $k_1/k_2 = 0.18$ at this point. Thus, the reticular lamina should move about 5.4 times more than the basilar membrane, in reasonable agreement with our data at this cochlear site.

As no sound stimuli were used in these experiments, we are

reporting the effects of outer hair cell forces in the absence of forward mechano-electrical transduction. Cochlear amplification switches in only when these movements are fed back to augment the sensory input to the hair cells[4-6]. Nevertheless, the cochlear responses reported here show comparable tuning to those induced by sound in a similar preparation[22] where a heterodyne interferometer, constructed around an optical sectioning microscope and sensitive to velocity, detected light backscattered from the cochlear partition. Our results support the hypotheses[4,6,20] that outer hair cells are responsible for amplification within the cochlea as well as for electrically evoked otoacoustic emissions from the intact cochlea[23], and show that it is possible to bridge the gap between *in situ*[24,25] experiments and *in vivo*[26-28] observations. □

Received 27 May; accepted 31 August 1993.

1. Brownell, W. E., Bader, C. R., Bertrand, D. & de Ripaubierre, Y. *Science* **227,** 194–196 (1985).
2. Dallos, P., Evans, B. N. & Hallworth, R. *Nature* **350,** 155–157 (1991).
3. Ashmore, J. F. *J. Physiol.* **388,** 323–347 (1987).
4. Neely, S. T. & Kim, D. O. *J. acoust. Soc. Am.* **79,** 1472–1480 (1986).
5. Dallos, P. in *Auditory Function: Neurobiological Bases of Hearing* (eds Edelman, G. M., Gall, W. E. & Cowan, W. M.) 153–188 (Wiley, New York, 1988).
6. Hubbard, A. *Science* **259,** 68–71 (1993).
7. Davis, H. *Hearing Res.* **9,** 79–90 (1983).
8. Mammano, F. & Ashmore, J. F. *J. Physiol.* **452,** 169P (1992).
9. Dallos, P. *Hearing Res.* **14,** 281–291 (1984).
10. Ashmore, J. F. & Meech, R. W. M. *Nature,* **322,** 368–371 (1986).
11. Evans, B. N., Hallworth, R. & Dallos, P. *Soc. Neurosci. Abstr.* **14,** 800 (1988).
12. Evans, E. F., Wilson, J. P. & Borerwe, T. A. 'Tinnitus', *Ciba Foundation Symposium* **85,** 108–138 (1981).
13. Stypulkowsky, P. H. *Hearing Res.* **46,** 113–143 (1990).
14. McFadden, D. & Plattsmier, H. S. *J. acoust. Soc. Am.* **76,** 443–448 (1984).
15. Shehata, W. E., Brownell, W. E. & Dieler, R. *Acta otolar.* **111,** 707–718 (1991).
16. Santos-Sacchi, J. *J. Neurosci.* **9,** 2954–2962 (1989).
17. Santos-Sacchi, J. *J. Neurosci.* **11,** 3096–3110 (1991).
18. Davis, H. *Laryngoscope* **68,** 359–382 (1958).
19. Kolston, P. J., de Boer, E., Viergever, M. & Smoorenberg, G. *J. acoust. Soc. Am.* **86,** 133–140 (1989).
20. Mammano, F. & Nobili, R. *J. acoust. Soc. Am.* **93,** 3320–3332 (1993).
21. Greenwood, D. D. *J. acoust. Soc. Am.* **87,** 2592–2605 (1990).
22. Ulfendahl, M., Khanna, S. M. & Flock, Å. *Hearing Res.* **40,** 55–64 (1989).
23. Hubbard, A. E. & Mountain, D. C. *Science* **222,** 510–512 (1983).
24. Reuter, G. & Zenner, H. P. *Hearing Res.* **43,** 219–230 (1990).
25. Reuter, G., Gitter, A., Thurm, U. & Zenner, H. P. *Hearing Res.* **60,** 236–246 (1992).
26. Sellick, P. M., Patuzzi, R. B. & Johnstone, B. M. *J. acoust. Soc. Am.* **72,** 131–141 (1982).
27. Ruggero, M. & Rich, N. *J. Neurosci.* **11,** 1057–1067 (1991).
28. Nuttall, A. L., Dolan, D. F. & Avinash, G. *Hearing Res.* **51,** 203–214 (1991).

ACKNOWLEDGEMENTS. We thank P. Kolston, M. Holley, M. Evans, R. Nobili and J. Gale for critical comments on the manuscript. This work was supported by the Wellcome Trust, the Wolfson Foundation, the EC and the Royal Society.

Inhibition of contractile vacuole function *in vivo* by antibodies against myosin-I

S. K. Doberstein*, I. C. Baines†, G. Wiegand‡, E. D. Korn† & T. D. Pollard*

* Department of Cell Biology and Anatomy, Johns Hopkins University School of Medicine, Baltimore, Maryland 21225, USA
† Laboratory of Cell Biology, National Heart Lung and Blood Institute, National Institutes of Health, Bethesda, Maryland 20892, USA
‡ Department of Medicine, Johns Hopkins University School of Medicine, Baltimore, Maryland 21225, USA

MYOSIN-I is thought to supply the force for movement of cell membranes relative to actin filaments (reviewed in refs 1, 2), but confirmation of this hypothesis has been difficult because of the presence of multiple isoforms of myosin-I and other unconventional myosins in most cells[3]. We report here the first evidence that a myosin-I isoform is essential for a specific class of intracellular membrane movements *in vivo*. In *Acanthamoeba*, the contractile vacuole is an autonomous structure which fuses with the plasma membrane to control the water content of the cell. Because myosin-IC is the only myosin-I isoform concentrated in the contractile vacuole complex[4,5], and a protein antigenically related to myosin-IC is located on or near the *Dictyostelium* (slime mould) contractile vacuole[6], we thought this organelle might provide the best opportunity to demonstrate a relationship between myosin-I and membrane motility. Antibodies that inhibit the activity of *Acanthamoeba* myosin-IC *in vitro* interfere with expulsion of excess water by the contractile vacuole *in vivo*, leading to overfilling of this organelle and cell lysis. Myosin-IC may generate the force required to contract the vacuole and may also be involved in transfer of water to the contractile vacuole during refilling.

Antibodies raised against a synthetic peptide with the sequence of the myosin-IC phosphorylation site[4] inhibited myosin-IC activity *in vitro* in three assays (Table 1): (1) phosphorylation of myosin-IC by the myosin-I heavy chain kinase (phosphorylation is required for activation of *Acanthamoeba* myosin-I ATPase activity[7,8] and motility *in vitro*[9,10]); (2) actin-activation of the Mg^{2+}-ATPase activity of prephosphorylated myosin-IC; and (3) crosslinking of actin filaments by myosin-IC, indicating that the ATP-sensitive actin binding site (which is near the antigenic epitope in the globular head) was blocked.

TABLE 1 Antibody inhibition of myosin I activities *in vitro*

Experiment	Antibody concentration (μM)	Activity (% of control) ATPase	Crosslinking	Phosphorylation
Myosin-IC	0.01	100	95	100
+	0.06	68	—	100
anti-myosin-IC	0.11	—	0	—
	0.63	0	—	87
	2.50	—	—	41
	3.13	—	—	3
	3.65	—	—	0
Myosin-IB	0.01	100	84	—
+	0.06	32	—	—
anti-myosin-IB	0.11	—	0	—
	0.63	0	0	—

Anti-myosin-IC IgG and anti-myosin-IB IgG were tested for inhibition of three activities: actin-activated Mg^{2+}-ATPase activity; crosslinking of F-actin; phosphorylation of myosin-I heavy chain. Myosin-I and myosin-I heavy chain kinase were purified by the method of Lynch *et al.*[27]. Actin was purified by the method of Spudich and Watt[23]. The Mg^{2+} ATPase activity of 0.2 μM myosin-I was assayed as described[24,25] in the presence and absence of 4 μM F-actin, with the basal activity in the absence of F-actin being subtracted to give the actin-activated Mg^{2+}-ATPase activity (control activity: 14.8 s^{-1}). Crosslinking of F-actin (4 μM) by myosin-I (0.2 μM) was measured by a pelleting assay using a low centrifugal force (18,500*g*) which was just sufficient for pelleting only crosslinked F-actin[26]. The mixture before pelleting and the supernatant after pelleting were analysed by SDS–PAGE and scanning densitometry to calculate the proportion of myosin-I present as F-actin crosslinks (control value: 100%). Myosin-IC (2μM) was phosphorylated by autophosphorylated myosin-I heavy chain kinase (60 nM); autophosphorylation is required for kinase activity[26]. Kinase was autophosphorylated by a 30 min incubation at 30 °C in 2.5 mM ATP, 3.5 mM $MgCl_2$, 2 mM EGTA, and 50 mM imidazole, pH 7.0. Myosin-I was phosphorylated in the same buffer supplemented with [γ-^{32}P]ATP (control activity: 1 mol P/mol myosin-I). Relative phosphorylation levels were determined by densitometer scans of autoradiograms after SDS–PAGE.

We used syringe loading[11] to introduce these antibodies into living *Acanthamoeba* cells. We added rhodamine–dextran to the loading solution, and isolated the loaded cells by fluorescence-activated cell sorting (Fig. 1). The combination of these two techniques is considerably easier than microinjection, particularly with *Acanthamoeba*[12], and rapidly yields a large population of loaded cells amenable to statistical analysis. Syringe-loaded anti-myosin-IC IgG was associated with the contractile vacuole